J Appl Physiol 103: 1837–1847, 2007.
First published August 30, 2007; doi:10.1152/japplphysiol.00542.2007.

Integration of jugular venous return and circle of Willis in a theoretical human model of selective brain cooling

Matthew A. Neimark,[1] Angelos-Aristeidis Konstas,[3,2] Andrew F. Laine,[1,2] and John Pile-Spellman[2]

Departments of [1]Biomedical Engineering and [2]Radiology, Columbia University, New York, New York; and [3]Department of Radiology, Massachusetts General Hospital, Boston, Massachusetts

Submitted 18 May 2007; accepted in final form 24 August 2007

Neimark MA, Konstas A-A, Laine AF, Pile-Spellman J. Integration of jugular venous return and circle of Willis in a theoretical human model of selective brain cooling. *J Appl Physiol* 103: 1837–1847, 2007. First published August 30, 2007; doi:10.1152/japplphysiol.00542.2007.—A three-dimensional mathematical model was developed to examine the induction of selective brain cooling (SBC) in the human brain by intracarotid cold (2.8°C) saline infusion (ICSI) at 30 ml/min. The Pennes bioheat equation was used to propagate brain temperature. The effect of cooled jugular venous return was investigated, along with the effect of the circle of Willis (CoW) on the intracerebral temperature distribution. The complete CoW, missing A1 variant (mA1), and fetal P1 variant (fP1) were simulated. ICSI induced moderate hypothermia (defined as 32–34°C) in the internal carotid artery (ICA) territory within 5 min. Incorporation of the complete CoW resulted in a similar level of hypothermia in the ICA territory. In addition, the anterior communicating artery and ipsilateral posterior communicating artery distributed cool blood to the contralateral anterior and ipsilateral posterior territories, respectively, imparting mild hypothermia (35 and 35.5°C respectively). The mA1 and fP1 variants allowed for sufficient cooling of the middle cerebral territory (30–32°C). The simulations suggest that ICSI is feasible and may be the fastest method of inducing hypothermia. Moreover, the effect of convective heat transfer via the complete CoW and its variants underlies the important role of CoW anatomy in intracerebral temperature distributions during SBC.

intracarotid saline infusion; intracerebral vascular flow rates; therapeutic hypothermia

THERAPEUTIC HYPOTHERMIA HAS been repeatedly shown to be effective in limiting central nervous system damage in animal models and clinical studies of ischemic stroke and cardiac arrest (6, 24). In most clinical studies, hypothermia is induced by surface cooling. Although this is the simplest and most cost-effective method of inducing hypothermia (13), it has two major limitations. First, surface cooling requires 3–7 h to reach the target brain temperature of 32–34°C (27, 41), although endovascular whole body cooling may be able to accelerate the induction of hypothermia (18). Second, whole body cooling methods are associated with several adverse effects such as impaired immune function, decreased cardiac output, pneumonia, and cardiac arrhythmias (13). Selective brain cooling (SBC) may be able to address both limitations of whole body cooling.

Different methods for SBC exist (21). The noninvasive methods most commonly used are cooling caps and helmets. However, theoretical analyses (8, 38, 46) and empirical measurements (7, 36, 51, 56) suggest that they are only effective in reducing the temperature in superficial cerebral regions and not deep brain structures. One potential method of SBC is intracarotid cold saline infusion (ICSI) in which cold saline is infused into the internal carotid artery (ICA) via transfemoral catheterization. This method is potentially much faster than whole body cooling and more effective than surface SBC. A recent theoretical study addressed the clinical feasibility of ICSI for inducing hypothermia (32). The theoretical analysis suggested that an infusion rate of 30 ml/min is sufficient to induce moderate hypothermia (defined as 32–34°C) within 10 min in the ipsilateral hemisphere. The theoretical model employed in this study, however, did not consider cooled jugular venous blood return to the body core, which should result in whole body temperature changes.

All the previous published theoretical analyses assume that blood from a particular feeding artery perfuses only a particular region in the brain, without mixing from the other source arteries (8, 32, 38). In reality, mixing of blood from different afferent vessels occurs within the circle of Willis (CoW). Blood can potentially flow from one hemisphere to another through the anterior communicating artery (ACoA) and from the ICA to the posterior cerebral artery (PCA) through the posterior communicating artery (PCoA). Intracerebral convective heat transfer through the CoW may affect the temperature response during ICSI. Furthermore, common variations in CoW anatomy exist such as a fetal P1 segment (fP1) of the PCA and a missing A1 segment (mA1) of the anterior cerebral artery (ACA) (37). Intracerebral temperature response may be different in these CoW variants (5).

The hypothesis of this study is that ICSI can selectively cool areas of the human brain and that spatiotemporal patterns of cooling will be affected by CoW anatomy and venous return. Our aim is thus to address three questions concerning the intracerebral temperature response to ICSI. First, what is the effect of jugular venous return on core temperature, and does a lower core temperature reinforce the induction of SBC? Second, how will redistribution of cooled ipsilateral ICA blood by the CoW affect the temperature response of the brain? Third, will variations in the CoW affect intracerebral temperature distributions? The impact of SBC on the distribution of cerebral blood flow (CBF) in the CoW is also examined.

GLOSSARY

Abbreviations

ACA	Anterior cerebral artery
ACoA	Anterior communicating artery
BA	Basilar artery
CoW	Circle of Willis
fP1	Fetal P1 segment of posterior cerebral artery
ICA	Internal carotid artery
Hct	Hematocrit

Address for reprint requests and other correspondence: Matthew A. Neimark, Dept. of Biomedical Engineering, Columbia Univ., 1210 Amsterdam Ave., New York, NY 10027 (e-mail: man2003@columbia.edu).

The costs of publication of this article were defrayed in part by the payment of page charges. The article must therefore be hereby marked "*advertisement*" in accordance with 18 U.S.C. Section 1734 solely to indicate this fact.

ICSI	Intracarotid cold saline infusion
mA1	Missing A1 segment of anterior cerebral artery
MAP	Mean arterial pressure
MCA	Middle cerebral artery
PCA	Posterior cerebral artery
PCoA	Posterior communicating artery
SBC	Selective brain cooling
SR	Shear rate
VA	Vertebral artery

Symbols

∇	Gradient operator
$\nabla\cdot$	Divergence operator
∂	Partial differentiation operator
$\iiint$	Volume integration
δ	Fraction of infused saline that remains in intravascular space
ρ	Density ($kg\cdot m^{-3}$)
π	$\approx$3.1416
η	Viscosity ($kg\cdot m^{-1}\cdot s^{-1}$)
Δ	Change from baseline
ω	Cerebral blood perfusion (s^{-1})
c	Heat capacity ($J\cdot kg^{-1}\cdot K^{-1}$)
d	Differentiation operator
D	Vessel diameter (m)
k	Heat conductivity ($W\cdot m^{-1}\cdot K^{-1}$)
m	Mass (kg)
n	Number of vessels entering a particular junction
q	Metabolism, heat production (W/m)
$\vec{r}$	Three-dimensional spatial location
t	Time (s)
F	Flow (m^3/s)
F	Vector of flows
G	Vascular conductivity ($kg^{-1}\cdot m^4\cdot s$)
G	Conductivity matrix
L	Vessel length (m)
P	Pressure ($kg\cdot m^{-1}\cdot s^{-2}$)
P	Vector of Pressures
T	Temperature (°C)
V	Volume

Subscripts

1,2	Arbitrary adjacent vessel junctions (P)
cACA	Contralateral anterior cerebral artery
cMCA	Contralateral middle cerebral artery
cPCA	Contralateral posterior cerebral artery
i	Arbitrary vascular junction (P), index corresponding to a vessel entering a vascular junction (F, T, ρ, c, Hct)
iACA	Ipsilateral anterior cerebral artery
iMCA	Ipsilateral middle cerebral artery
iPCA	Ipsilateral posterior cerebral artery
B	Combined basilar and vertebral (G)
IV	Intravascular
IV0	Baseline intravascular
RBC	Red blood cell

MATERIALS AND METHODS

Heat transfer model. Heat transfer was simulated in a three-dimensional hemispherical mathematical model, developed in spherical coordinates, and consisting of four separate tissue layers: white matter, gray matter, bone, and skin (Fig. 1, *A* and *B*). Physical and physiological properties, as published in previous studies, were used for each of the tissue layers, blood, and saline (Table 1) (32). Heat transfer develops over space and time according to the Pennes bioheat equation (39):

$$\frac{\partial T(\vec{r},t)}{\partial t} = \frac{\nabla\cdot[k(\vec{r})\nabla T(\vec{r},t)]}{\rho(\vec{r})c(\vec{r})} + \frac{\rho_{blood}c_{blood}}{\rho(\vec{r})c(\vec{r})}\omega(\vec{r},t) \times [T_{artery}(\vec{r},t) - T(\vec{r},t)] + \frac{q(\vec{r},t)}{\rho(\vec{r})c(\vec{r})} \quad (1)$$

where T is temperature (of tissue when not subscripted), k is the tissue thermal conductivity, ρ is density, c is heat capacity, ω is blood perfusion, q is tissue metabolism, t is the time point, and $\vec{r}$ is the spatial location. All blood has core temperature except for the ipsilateral ICA, whose temperature is

$$T_{ICA} = \frac{\rho_{blood}c_{blood}\text{ICA Blood Flow}\cdot T_{core} + \rho_{saline}c_{saline}\text{Saline Flow}\cdot T_{saline}}{\rho_{blood}c_{blood}\text{ICA Blood Flow} + \rho_{saline}c_{saline}\text{Saline Flow}} \quad (2)$$

ICSI of 30 ml/min was used in all simulations.

In a transfemoral catheterization, outflow temperature of the ICA, T_{saline}, will be higher than at the point of inflow because of body warming. Catheter outflow temperature was thus experimentally determined by using a life-size phantom model of the human arterial tree. A 5F endovascular catheter entered the model in the femoral bifurcation and ended in the ICA. Water at 37°C was pumped continuously through the model while freezing-cold saline was injected into the catheter and the outlet catheter temperature, T_{saline}, was monitored with a fluoroptic temperature probe and determined to be 2.8°C for a saline flow rate of 30 ml/min (32).

For brain tissue, metabolism is a function of temperature and perfusion is a function of temperature and hematocrit (32) according to

$$q = q_0\cdot 3.0^{0.084(T-37)} \quad (3)$$

$$\omega = \omega_0\cdot 3.0^{0.084(T-37)}(1 - 2.2\Delta_{Hct}) \quad (4)$$

The coefficients in *Eqs. 3* and *4* were derived by fitting data points from PubMed-indexed experimental studies, reviewed elsewhere (32). The root mean square error between the data points and the function was minimized by varying the coefficients through the unconstrained nonlinear optimization.

ICSI limited the amount of intracarotid blood flow in *Eq. 2* according to

$$\text{ICA Blood Flow} = \text{ICA Total Flow} - \text{Saline Flow} \quad (5)$$

where ICA Total Flow is the flow rate of perfusate in the ipsilateral ICA determined directly by integrating corresponding perfusion territories. *Equation 5* states that cerebral autoregulation keeps CBF relatively constant notwithstanding additional pressure from the infusion pump, instead of the saline infusion adding to the total flow of the ICA and CBF of the corresponding perfusion territories as in a previous theoretical study (32). Hydrodynamic circuit models reveal that so long as cerebral vascular resistance significantly exceeds vascular resistance upstream from the pump (i.e., in the aorta and common carotid arteries) the infusion pump will not add significant flow to the ICA.

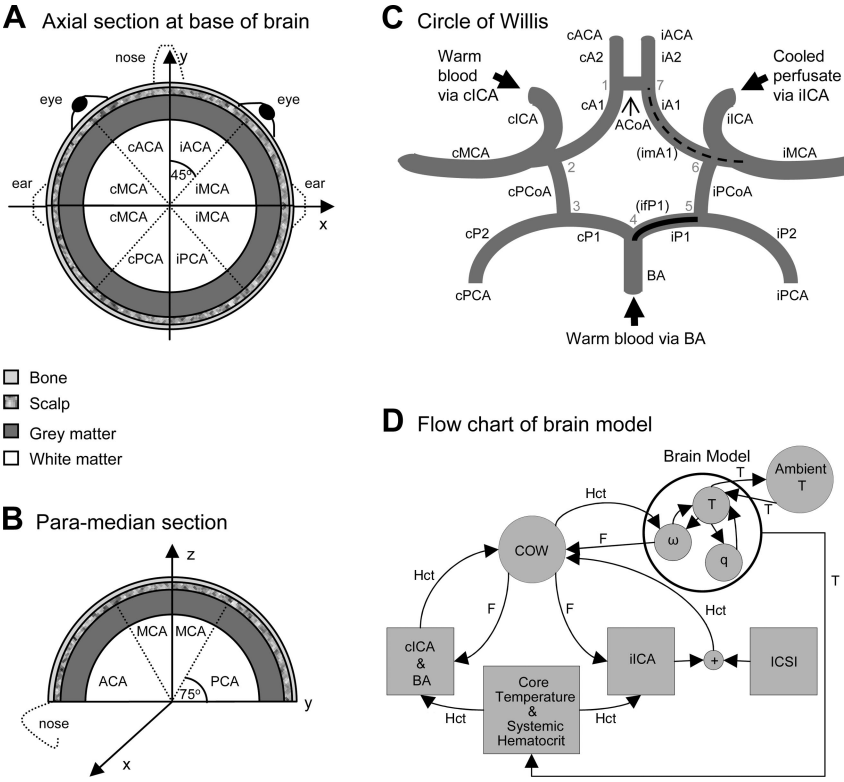

Fig. 1. Anatomic layout of the head model. *A*: axial section at the base of the brain with the demarcation of the vascular territories. The letters i and c prior to the vessel abbreviation signify, respectively, the side either ipsilateral or contralateral to the infused vessel. *B*: paramedian section of the model. *C*: simplified 2D circle of Willis geometry. Vessels are either ipsilateral or contralateral to the site of cooled perfusate inflow. Of the circle of Willis variants, only the imA1 (dotted line) and the ifP1 (solid black line) are illustrated. The numbers 1–7 (in gray) correspond to the subscripted numbers in *Eq. 13*. *D*: flowchart of the brain model.

Effect of infusion volume on hematocrit. When the bloodstream is infused with isotonic saline, part of it enters the extravascular space and part of it is removed by the kidneys. The remaining volume of saline hemodilutes the blood. An expression for the resulting change of hematocrit is given as follows (32):

$$\Delta_{Hct} = \frac{\delta V_{RBC} \Delta V_{IV}}{V_{IV0}(V_{IV0} + \delta \Delta V_{IV})} \quad (6)$$

where V_{RBC} is the total red blood cell volume, V_{IV0} is the initial total intravascular volume (including V_{RBC}), ΔV_{IV} is the volume of added saline, and δ is the fraction of infused water that remains intravascular (i.e., does not end up in the extravascular space and is not removed by the kidneys). An initial hematocrit of 42% and an initial $V_{IV0} = 5.0$ liters is assumed (implying $V_{RBC} = 2.1$ liters).

$\delta = 0.42$ was determined in a previous study (32) by fitting *Eq. 6* by unconstrained nonlinear optimization with published experimental hypervolemic hemodilution data (19, 20, 26, 28, 45, 52, 53).

For the territory of the brain perfused by the ipsilateral ICA, the values of hematocrit (which affects perfusion) had to be modified because of the cold saline infusion. An expression for the local dilution effect of the infusion is given by

$$Hct_{local} = \frac{\text{ICA Blood Flow} \cdot Hct}{\text{ICA Blood Flow} + \text{Saline Flow}} \quad (7)$$

Incorporation of venous return. Since blood and brain tissues achieve thermal equilibrium (2), venous return temperatures were calculated by integrating the product of the brain temperature and blood perfusion over the entire brain model as follows (14):

$$T_{venous} = \iiint_{\text{Brain Model}} \omega(\vec{r}) T(\vec{r}) d\vec{r} \Big/ \iiint_{\text{Brain Model}} \omega(\vec{r}) d\vec{r} \quad (8)$$

T_{venous} is the average venous return temperature.

Equilibration of venous blood with the body core temperature (T_{core}) will decrease T_{core} (54):

Table 1. *Physical and physiological properties in the model (modified from Ref. 32)*

Anatomic Structure of the Head	Specific Heat *c*, J/kg K	Mass Density ρ, kg/m^3	Thermal Conductivity *k*, W/m K	Perfusion ω_0, ml/(min·100 g)	Metabolic Rate q_0, W/m^3	Radius *r*, mm
Saline	4,213	1,006	0.5	N/A	N/A	N/A
Blood	3,800	1,050	0.5	N/A	N/A	N/A
Scalp	4,000	1,000	0.342	2.0	363.4	93
Bone	2,300	1,520	1.16	1.8	368.3	89
Gray matter	3,700	1,030	0.49	80	16,700	85
Whitematter	3,700	1,030	0.49	20	4175	67

N/A, not applicable.

$$\frac{dT_{core}}{dt} = \frac{\rho_{blood} c_{blood}(T_{venous} - T_{core}) \iiint_{Brain\ Model} \omega(\vec{r})d\vec{r}}{m_{body} c_{body}} \quad (9)$$

where $m_{body} = 70$ kg is body mass and $c_{body} = 3{,}475\ J \cdot kg^{-1} \cdot K^{-1}$. In this study, the body core is modeled as a compartment separate from the brain with uniform temperature that is affected only by the blood temperature returning from the brain model. See APPENDIX for a derivation of this equation. See also DISCUSSION.

CoW model. Representative values averaged from published human data of CoW vessels were used to simulate individual vessels in the present CoW model (12, 37, 47). Representative values for vessels in complete CoW, as well as vessels in CoW with mA1 segment of ACA or fP1 segment of PCA are summarized in Table 2. Modeling of the CoW was performed with a linear model (5, 22). According to Poiseuille's law, the flow in a vessel is determined as follows:

$$F = G(P_2 - P_1) \quad (10)$$

where F is the flow, P_2 and P_1 are the pressures at the two ends of the vessel, and G is the flow conductance. G itself is determined by

$$G = \frac{\pi D^4}{128 \eta_{blood} L} \quad (11)$$

where η_{blood} is blood viscosity, L is vessel length, and D is vessel diameter. The hemispheric model was divided up into six perfusion territories corresponding to each of the cerebral arteries (Fig. 1, *A–C*). These vascular territories were chosen to correspond roughly to both perfusion regions recently reported in selective arterial spin labeling perfusion studies (48) and cerebral artery blood flow proportions described in various studies (11, 12, 47). Flow rates through the CoW afferent arteries were determined by integrating the ω values in the corresponding perfusion territories in Fig. 1, *A* and *B* (and calculated using *Eq. 4*) according to

$$F = \iiint_{Territory} \omega dV \quad (12)$$

Blood flows in the CoW and supply vessels (i.e., ICAs and BA) were determined by Kirchoff's circuit laws, which state that the sum of incoming flows toward an arterial junction is zero and the sum of pressure changes in a closed arterial circuit is zero. In this manner, the CoW afferent vessels act as flow sources and pressures at the origins of the ICAs and BA were clamped to mean arterial pressure. The set of Kirchoff's law equations is expressed by the following matrix equation, which was used to determine the pressure values P_i:

$$\begin{bmatrix} -G_{12}-G_{17} & G_{12} & 0 & 0 & 0 & 0 & G_{17} \\ G_{12} & -G_{12}-G_{23}-G_{ICA} & G_{23} & 0 & 0 & 0 & 0 \\ 0 & G_{23} & -G_{23}-G_{34} & G_{34} & 0 & 0 & 0 \\ 0 & 0 & G_{34} & -G_{34}-G_{45}-G_{BA} & G_{45} & 0 & 0 \\ 0 & 0 & 0 & G_{45} & -G_{45}-G_{56} & G_{56} & 0 \\ 0 & 0 & 0 & 0 & G_{56} & -G_{56}-G_{67}-G_{ICA} & G_{67} \\ G_{17} & 0 & 0 & 0 & 0 & G_{67} & -G_{17}-G_{67} \end{bmatrix} \times \begin{bmatrix} P_1 \\ P_2 \\ P_3 \\ P_4 \\ P_5 \\ P_6 \\ P_7 \end{bmatrix} = \begin{bmatrix} F_{cACA} \\ F_{cMCA} - MAP \cdot G_{ICA} \\ F_{cPCA} \\ -MAP \cdot G_B \\ F_{iPCA} \\ F_{iMCA} - MAP \cdot G_{ICA} \\ F_{iACA} \end{bmatrix} \quad (13)$$

The conductance values in this equation were calculated according to *Eq. 11*. Subscripted numbers represent points along the CoW (Fig. 1*C*) and the vessels between them (double digits). MAP = 95 mmHg is mean arterial pressure. G_{ICA} is the conductance of the ICA and G_B is the combined conductance of the vertebral and basilar arteries.

After solving for all the P_i values of the CoW, flow values in all the CoW and source vessels were calculated according to *Eq. 10*. The combination of flows in the CoW allowed the calculation of temperature and hematocrit for each of the vessels in the model. For every junction of vessels, *Eq. 10* was used to determine which vessels had flows entering

Table 2. *Length and diameters of vessels in complete CoW, mA1, and fP1 models (averaged from Refs. 12, 37, 47)*

(mm)	ICA	BA	VA	iA1	cA1	ACoA	iP1	cP1	iPCoA	cPCoA
L	225	30	225	13.8	13.8	2.7	7.2	7.2	13.3	13.3
$D_{complete}$	3.57	3.24	2.71	1.95	1.95	1.40	1.82	1.82	1.14	1.14
D_{mA1}	3.57	3.24	2.71	0.16	2.33	2.33	1.79	2.14	1.74	1.66
D_{fP1}	3.57	3.24	2.71	1.99	2.30	1.63	1.30	2.61	2.01	2.08

L, vessel length; $D_{complete}$, vessel diameter in complete CoW; D_{mA1}, vessel diameter in CoW with mA1; D_{fP1}, vessel diameter in CoW with fP1; the letters i and c prior to the vessel abbreviation represent ipsilateral and contralateral sides of the CoW.

or exiting the junction. The temperature and hematocrit of each vessel flow exiting the junction mix was calculated according to

$$T = \frac{\sum_{i=1}^{n} T_i F_i \rho_i c_i}{\sum_{i=1}^{n} F_i \rho_i c_i} \quad (14)$$

$$Hct = \frac{\sum_{i=1}^{n} Hct_i F_i}{\sum_{i=1}^{n} F_i} \quad (15)$$

Temperature in each of the CoW vessels was determined by using the temperatures of the source vessels (i.e., ICAs and BA), acquired from *Eqs. 2* and *9*. Ultimately, the temperature of each CoW efferent (i.e., ACA, MCA, PCA) was calculated by using *Eq. 14* and was used as the arterial temperature in *Eq. 1* to propagate the brain temperature. This temperature was also used in *Eqs. 3* and *4* to determine brain perfusion and metabolism for *Eq. 1*. Similarly, hematocrit of each of the source vessels was determined by *Eqs. 6* and *7*. Hematocrit in the remaining CoW vessels and CoW efferents was determined with *Eq. 15*. Hematocrit values from CoW efferents were used in *Eq. 4* to determine brain perfusion for the corresponding territories.

Blood viscosity was dependent on the temperature, hematocrit, and shear rate (SR) (10):

$$\eta_{blood} = \left(e^{\frac{9.21}{SR} + 0.0137 \cdot Hct} \right) \left[1.74 + \frac{9.78}{1 + e^{0.28(T - 15.2)}} \right] \quad (16)$$

Shear rate, a function of blood velocity and vessel diameter, was determined (23) according to

$$SR = \frac{32F}{\pi D^3} \quad (17)$$

At every iterative step, the vascular resistance of each vessel was recalculated according to *Eq. 16* and *Eq. 11*. The resistive matrix in *Eq. 13* was also reevaluated to determine pressures and flows in the CoW.

Figure 1*D* shows a flowchart demonstrating relationships between all model components and parameters. Simulations were performed in MATLAB by using the same grid spacing, temporal spacing, and overall numerical procedure as from a previous study (32).

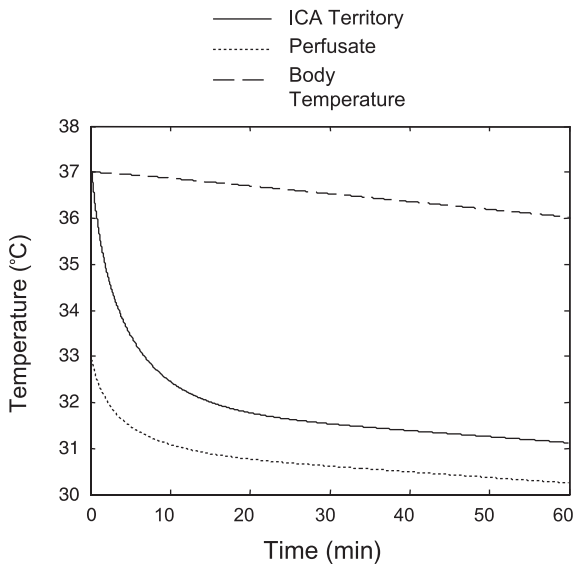

Fig. 2. Effect of ICSI (T = 2.8°C, F = 30 ml/min) on transient temperature profile of ipsilateral ICA territory and ICA perfusate for non-CoW model with integration of jugular venous return.

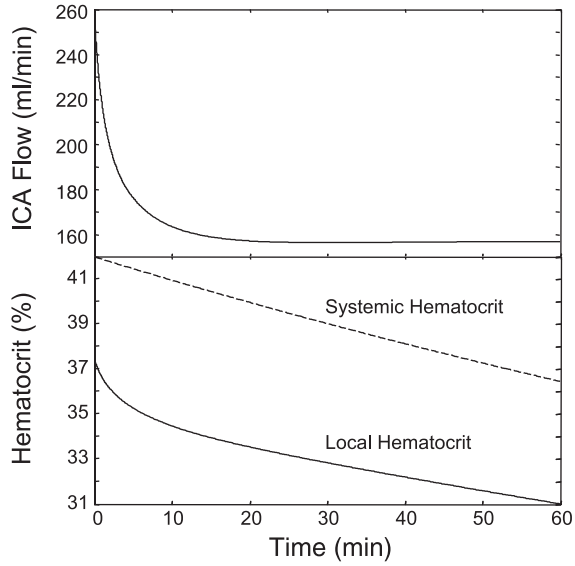

Fig. 3. Effect of ICSI on the ICA blood flow rate (not including 30 ml/min saline infusion) and on hematocrit. Both the systemic hematocrit and the local (i.e., perfusate) hematocrit are shown.

RESULTS

Effect of ICSI in the venous return model. Figure 2 examines the effect of ICSI at a rate of 30 ml/min on the transient temperature profile of a human brain model incorporating jugular venous return. There was a two-phase decrease in ipsilateral ICA territory temperature. The initial fast phase cooled the ICA territory temperature to therapeutic levels (34°C) in ~5 min. The sustained phase of cooling resulted in a slower continuous cooling of the ipsilateral ICA territory, reaching a minimum temperature of 31.1&cjs0148;C after 60 min of ICSI blood flow rate (not including 30 ml/min infusion (Fig. 3). Systemic hematocrit decreased from 42 to 37.5% over the course of the infusion whereas local hematocrit decreased from 37 to 31%. Figure 4*A* illustrates the spatial temperature distribution after 60 min of ICSI in the venous return model. Inclusion of jugular venous return had a mild cooling effect in the rest of the brain. Body temperature fell by ~1°C after 1 h of infusion. In Fig. 6, body temperature from the venous return ICSI model is compared with a similar 30 ml/min venous infusion model of 2.8°C saline. Body temperature in the two models is similar although the venous return ICSI temperature is slightly higher. This temperature difference is reflected in lower brain temperatures observed in the ICSI model.

CoW model: baseline flow rates. Table 3 shows flow rates for the ipsilateral ICA, contralateral ICA, and basilar artery (BA) at baseline (i.e., before cold saline infusion) for three separate models: The complete CoW, mA1 CoW, and fP1 CoW. The baseline flow rate values are compared with values from three other studies. Two of these studies utilized phase-contrast magnetic resonance angiography to obtain in vivo flow rates from subjects, and one study employed a nonlinear vascular flow model. The baseline flow rates in the feeding arteries of the present model were within the range of values reported in the literature.

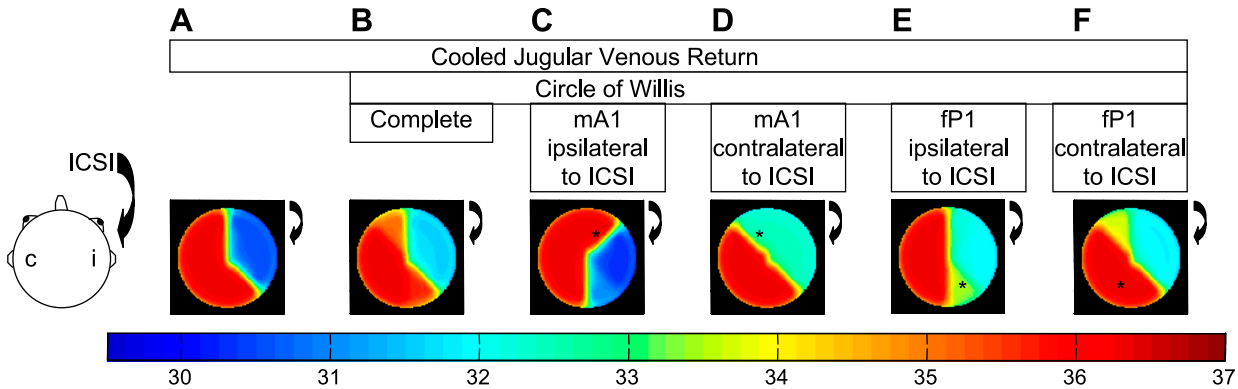

Fig. 4. Axial sections of the brain 4.5 cm from the base with the spatial temperature distribution 60 min after ICSI. Diagram of head on left illustrates corresponding anatomical locations of temperatures. The black arrow shows the side of ICSI. *A*: model with venous return only. *B*: model with complete CoW (includes venous return). *C*: CoW model with mA1 ipsilateral to ICSI. *D*: CoW model with mA1 contralateral to ICSI. *E*: CoW model with fP1 ipsilateral to ICSI. *F*: CoW model with fP1 contralateral to ICSI. Asterisks represent the approximate position of each variant vessel (mA1 or fP1).

Complete CoW model: effect of ICSI on brain temperature and CBF distribution. The transient temperature profile of the ICA territory in the model incorporating the jugular venous return and complete CoW model was similar to that for the venous return model without the CoW. However, the spatial temperature distribution maps reveal two differences between the two models (Fig. 4, *A* and *B*). First, the ipsilateral ICA territory was cooled less in the complete CoW, though it remained well within the potentially therapeutic temperature range. Second, the temperatures of the ipsilateral PCA territory and the contralateral ACA territory were mildly hypothermic (≤35.5°C). No appreciable cooling below body core temperature was achieved in the corresponding territories of the jugular venous return model.

For the complete CoW, the afferent blood supply was split symmetrically between the ipsilateral and contralateral afferent arteries with the ICAs supplying 3.5 times as much blood as the BA at the onset of ICSI and 3.2 times after 1 h of ICSI. Before infusion of cold saline, there was no blood flow through the ACoA and only a small flow through the PCoAs (Fig. 5*A*). Also, the ICAs contributed to the blood supply of the PCA territories since the direction of flow through the PCoAs was from anterior to posterior. ICSI resulted in an asymmetrical afferent blood supply. Total flow was reduced more in the ipsilateral ICA than the contralateral ICA (225 vs. 250 ml/min). Another notable observation was that ICSI caused a 20 ml/min ipsilateral-to-contralateral flow through the ACoA.

CoW with a mA1 segment of ACA: effect of ICSI on brain temperature and CBF distribution. The main difference between the model with a mA1 segment of ACA and the complete CoW model was the diameter of A1. The mA1 had a diameter of 0.16 mm compared with the usual A1 diameter of 1.95 mm in the complete CoW model (Table 2). In subjects with a mA1 segment, the missing segment may be either ipsilateral or contralateral to the infused ICA. Compared with the complete CoW model, ICSI in the same side as the mA1 segment (ipsilateral mA1 model) resulted in a deeper level of hypothermia in the ipsilateral middle cerebral artery (MCA) territory (30.5 vs. 32°C) and an induction of therapeutic-level hypothermia in the ipsilateral PCA territory (Fig. 4*C*). However, the ipsilateral ACA territory was not cooled. There was an asymmetrical blood supply in the steady-state ipsilateral mA1 model. The ipsilateral mA1 had effectively no blood flow, whereas blood flow was almost doubled in the contralateral A1 segment compared with the contralateral A1 in the complete CoW model (Fig. 5*B*). Ipsilateral ICA blood flow was 30% less than contralateral ICA flow, and a significant proportion of the contralateral ICA flow was directed to the ipsilateral ACA via the ACoA.

ICSI to the opposite side from the mA1 segment (contralateral mA1 model) produced a markedly different distribution of hypothermic temperatures in the brain. A uniform level of cooling (32.5°C) was achieved in the contralateral ACA, ipsilateral ACA, and ipsilateral MCA territories (Fig. 4*D*). The ipsilateral PCA territory did not cool. Cooled ipsilateral ICA blood was directed to the ipsilateral ACA and the contralateral ACA via the ipsilateral A1 segment and the ACoA, leading to hypothermia in the ipsilateral ACA and contralateral ACA territories. The direction of blood flow in the ipsilateral PCoA was from posterior to anterior (Fig. 5*C*).

Table 3. *Comparison of CoW feeding vessel flow rates between the present model and published data*

	Volume Flow Rate, ml/min								
	Complete CoW			CoW with mA1			CoW with fP1		
	iICA	cICA	BA	iICA	cICA	BA	iICA	cICA	BA
Tanaka et al. (47)	311±73	304±74	165±43	236±48	367±67	141±39	355±66	317±60	90±24
Hendrikse et al. (21a)				214±94	303±56	104±36	272±66*	272±66*	91±25
Moore et al. (37)	270	270	210	222	321	204	300	291	162
Current model	270	270	158	227	320	150	283	270	144

Values for experimental studies are given as means ± SD. *Ipsilateral and contralateral values were averaged.

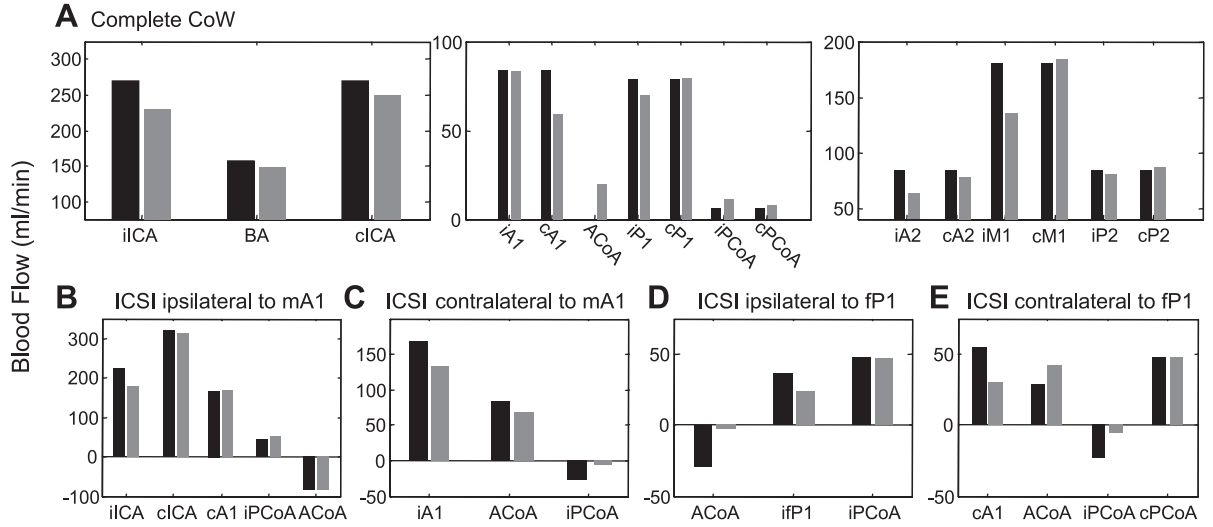

Fig. 5. Blood flow rate through major cerebral arteries before ICSI (black) and after 60 min of ICSI (gray). *A*: comprehensive illustration of major cerebral arteries in the complete CoW model. *B–E*: selected cerebral arteries in CoW model with mA1 ipsilateral to ICSI (*B*); CoW model with mA1 contralateral to ICSI (*C*); CoW model with fP1 ipsilateral to ICSI (*D*); and CoW model with fP1 contralateral to ICSI (*E*). M1 refers to the M1 segment of the MCA; P1 and P2 refer to the P1 and P2 segments of PCA; A1 and A2 refer to A1 and A2 segments of ACA. Ipsilateral ICA flow includes 30 ml/min of saline infusion.

CoW with a fP1 segment of PCA: effect of ICSI on brain temperature and CBF distribution. The main difference between the model with a fP1 segment of PCA and the complete CoW model was the diameter of P1. The fP1 had a diameter of 1.30 mm compared with the usual P1 diameter of 1.82 mm in the complete CoW model (Table 2). In subjects with a fP1 segment, the hypoplastic vessel may be ipsilateral (ipsilateral fP1 model) or contralateral (contralateral fP1 model) to the infused hemisphere. The ipsilateral ICA territory reached a similar level of hypothermia after ICSI in the ipsilateral fP1 model as in the complete CoW model. However, the ipsilateral PCA territory reached lower hypothermic temperatures in the ipsilateral fP1 model than in the complete CoW model (33.5 vs. 35.5°C, see Fig. 4*E*). At the same time, the contralateral ACA territory temperature was not cooled. Also, there was nearly five times the blood flow through the ipsilateral PCoA compared with the contralateral CoW, following the same anterior-to-posterior direction (Fig. 5*D*). Another notable feature was the significant contralateral-to-ipsilateral flow (30 ml/min) in the ACoA (which was eliminated by ICSI) resulting in the inability of ICSI to cool the contralateral ACA territory.

ICSI in the contralateral fP1 model cooled the ipsilateral ICA territory (32°C) and the contralateral ACA territory, the latter reaching lower temperatures than the contralateral ACA territory in the complete CoW model (34 vs. 35°C). The ipsilateral PCA territory did not cool (Fig. 4*F*). Blood was diverted from the contralateral ICA to the contralateral PCA at 50 ml/min through the contralateral PCoA to supply the contralateral PCA territory (Fig. 5*E*). The diversion of blood away from the anterior circulation halved the flow in the contralateral A1 segment, compared with the corresponding A1 segment of the ipsilateral fP1 model.

DISCUSSION

Novel aspects of the present model. The present theoretical model has several novel aspects. First, the effect of cooled jugular venous return on body core temperature is modeled. Thus core blood temperature is not clamped at 37°C as in the nonvenous return model (32) but continuously changes according to cooled venous blood that returns from the brain. Second, intracerebral convective heat transfer through the CoW is modeled and its effect on brain temperature distribution in the human brain is examined. Previously published heat transfer models attribute intracranial heat transfer to conduction only (8, 32, 38, 44, 54, 55). Third, two common CoW variants are simulated and their role in intracerebral temperature distribution is examined. The model also allows for an analysis of the impact of SBC on the CBF distribution in the CoW. Baseline flow rates for the CoW model for the complete CoW and two variant types compared with three other studies strongly suggest the model's ability to accurately represent arterial flow rates.

Comparison of venous return model to nonvenous return model. In the present study, perfusate temperature and brain temperature in the ICA territory continued to decrease even after the initial fast phase of cooling was completed. This is in contrast to a previous theoretical study of ICSI (32) where venous return was omitted from the model. In this previous study ipsilateral ICA territory temperature demonstrated a similar initial fast cooling phase but then started gradually increasing after the end of the fast phase. Similarly, at the point at which the ICA and perfusion temperatures began increasing, the ICA flow rate also began increasing. This was explained by hemodilution. In the present study, which accounted for core body cooling by venous return, the ICA flow rate leveled off (Fig. 3), indicating that the effect hemodilution, which increases blood flow, was counteracted by the effect of lower brain temperatures according to *Eq. 4*.

CoW blood flows and cooling patterns. There was a wide variation of spatiotemporal cooling patterns based on which CoW variant was modeled. For the complete CoW, mild hypothermia (35°C) was observed in the contralateral territory of the ACA. This can be explained by the both the ipsilateral-to-contralateral cold flow through the ACoA and the resulting

reduced flow of warm blood through the contralateral A1 segment (Fig. 4*B*). For the CoW with a missing A1 segment ipsilateral to ICSI, the territory of the ipsilateral ACA was not cooled at all because the cooled perfusate through the ipsilateral ICA could not be communicated to the ipsilateral ACA, and therefore this vessel received its entire blood supply from the warm contralateral side. Because all the cooled perfusate was transmitted to the ipsilateral MCA and PCA territories, these regions cooled more than in the complete CoW case. For the contralateral fetal P1 CoW, there was greater cooling in the contralateral ACA territory than in the complete CoW case (34 vs. 35°C). However, the ipsilateral PCA territory did not cool at all. These results can be explained by the high resistance of the contralateral P1 diverting flow from the BA to the ipsilateral side and causing a posterior-to-anterior flow through the ipsilateral PCoA ensuring that the ipsilateral PCA region would not be cooled. This in turn caused a greater ipsilateral-to-contralateral flow through the ACoA, cooling the contralateral ACA region.

Implications of the results. The results of the present study have several physiological and clinical implications. Cooled jugular venous return influenced SBC by reducing the temperature of the ipsilateral ICA territory and each of the other territories by an additional 1°C after 60 min of ICSI. The additional brain temperature decrease reflected the corresponding body core temperature drop. The mild core cooling facilitated SBC, yet body temperatures never reached levels at which adverse effects of whole body hypothermia occur (13). Indeed, mild systemic hypothermia as observed in our study is not entirely unwanted because it could help maintain SBC at lower cold saline infusion rates after target temperature is reached without imparting aforementioned deleterious side effects of systemic hypothermia.

The complete CoW allowed for interhemispheric and ipsilateral ICA-to-PCA convective transfer of the cooled ipsilateral ICA blood, mildly cooling the contralateral ACA and ipsilateral PCA territories. The mA1 and fP1, two common CoW variants, allowed for sufficient cooling of the ipsilateral MCA territory but produced very different results regarding the ipsilateral ACA, contralateral ACA, and ipsilateral PCA territory temperatures, depending on the anatomical variant and its relation to the site of ICSI. The influence of the convective heat transfer via the complete CoW and its variants underlies the importance of including it in hypo- and hyperthermic brain models. It also suggests that in animal experiments of brain cooling, temperature recordings should be obtained from all major perfusion territories and not just from one or two, as has been done in the past (9, 42).

The model predicts that therapeutic hypothermic levels can be potentially achieved after 5–10 min of ICSI. This would be 18 to 84 times faster than the 3–7 h needed for whole body cooling through noninvasive methods (27, 41) and 10 to 30 times faster than whole body endovascular cooling (18). Furthermore, the failure of noninvasive SBC methods in inducing hypothermia (7, 36, 51) makes ICSI the only potential method of rapidly inducing hypothermia. It is well established that the therapeutic window, i.e., the time period in which ischemic stroke can be treated, is around 3 h (31). Hence, ICSI has important clinical implications as it is the only potential method of hypothermia induction with the ability to cool the ipsilateral brain fast enough so as to not miss the therapeutic window. Furthermore, rapid induction of hypothermia with ICSI may lengthen the therapeutic window and allow a combination with techniques that aim at restoring the blood circulation, like local intra-arterial thrombolysis or mechanical thrombectomy. Other drugs commonly used to manage secondary complications of ischemic stroke could be infused through the catheter administering ICSI (43). The model suggests that there are significant blood flow changes in the CoW after inducing hypothermia and changes in flow distributions occur with variations in the CoW anatomy. The derived blood flow values for each CoW vessel may allow for adjustments in the doses of drugs coadministered with ICSI according to the each subject's CoW anatomy.

The present model predicts that 60 min of ICSI at 30 ml/min decreases the local hematocrit to 30.6%. Extensive experience with cardiopulmonary bypass operations established hematocrit values in the very low 20s as the lowest acceptable levels in terms of safety (35). From a clinical applicability point of view, the theoretical maximum safe duration of hypothermia maintenance with ICSI can be up to 3 h, since, by extrapolating the local hematocrit curve in Fig. 3, the model suggests it takes around 3 h to reach hematocrit values in the low 20s. Postischemic hypothermia in humans must be maintained for a minimum of 6–12 h to be effective (24). Hence a potential role of ICSI in the acute management of ischemic stroke is for rapid induction of hypothermia, whereas mild systemic hypothermia via surface or endovascular whole body cooling can maintain hypothermia.

Confirmation of body cooling in jugular venous model. Through *Eq. 9*, the jugular venous model makes an assumption that core temperature will be affected only by cool blood returning from the brain. In reality, body temperature could increase through shivering or decrease through heat loss to the environment. Our assumption is based on the observation that, in normal temperature homeostasis, bodily heat sources and losses balance one another out to maintain a constant temperature and therefore, for temperature changes resulting from the addition of a heat sink such as a cold infusion, heat loss to the environment will also be matched by any metabolic sources of heat.

This assumption is confirmed with data from eight direct intravascular (IV) cold fluid infusion studies (11 groups of patients, Table 4). The temperature drop from such an infusion is employed with the following equation (see APPENDIX):

$$\frac{dT_{core}}{dt} = \frac{\rho_{blood} c_{blood} (T_{infusion} - T_{core}) F_{infusion}}{m_{body} c_{body}} \quad (18)$$

This equation is completely analogous to *Eq. 9* and also does not include terms for metabolic sources or heat losses to the environment.

Figure 6 shows the body core temperature drop in the model from venous return compared with the body core temperature drop that would incur, according to *Eq. 18*, from an equivalent IV infusion of the same temperature and flow rate (30 ml/min). As expected, the resultant temperature from the IV infusion is slightly lower than in the venous return model because in the venous return model the brain temperature remains lower than in the rest of the body. However, the temperature difference between the venous return and IV infusion curves remains less than 0.1°C because the brain model mass (1.8 kg) is only 2.5%

Table 4. *Compilation of IV cold fluid infusion studies*

Study	Subjects	Method	Drugs Administered	$V_{infusion}$, ml	Infusion Rate, ml/min	Observed Temperature Drop, °C	Predicted Temperature Drop, °C
Bernard et al. (4)	22 comatose elderly CA patients	4°C LRS in peripheral or CVL	vecuronium, midazolam	2,100	70	1.6	1.12
Baumgardner et al. (3)	6 elderly neurosurgical patients	4°C 5% albumin peripheral	thiopental, vecuronium, fentanyl	375	12.5	0.6	0.21
Badjatia et al. (1)	9 elderly neurological patients with fever	4°C NS peripheral	none	2,160	36	2.1	1.28
Frank et al. (15)	10 healthy young men	4°C LRS via CVL	none	3,830	128	1	2.08
Rajek et al. (40)	9 healthy young men	4°C NS via CVL	propofol, vecuronium, isoflurane	2,880	96	2.5	1.58
Rajek et al. (40)	9 healthy young men	20°C NS via CVL	propofol, vecuronium, isoflurane	2,880	96	1.4	0.82
Frank et al. (16)	9 healthy young men	4°C NS via CVL	none	2,100	70	1.1	1.17
Frank et al. (16)	9 healthy young men	4°C NS via CVL	none	2,800	93	1.3	1.54
Kim et al. (29)	17 comatose elderly CA patients	4°C NS peripheral	midazolam, vecuronium				
Frank et al. (17)	8 healthy elderly subjects	4°C NS CVL	none	1,800	60	1.6	1.01
Frank et al. (17)	8 healthy young subjects	4°C NS CVL	none	1,800	60	1	1.01

CA, cardiac arrest; CVL, central venous line; LRS, lactated Ringer's solution; NS, normal saline.

of the body's mass. This demonstrates that infusing the body through the carotids yields a similar bodily temperature change as an IV infusion. However, brain temperature decreases are much greater via the intracarotid route.

Table 4 summarizes the IV infusion studies and includes the reported temperature drops from the studies along with the predicted temperature drops according to *Eq. 18*. The average temperature difference between the actual and predicted drop (actual minus predicted) was 0.24°C (standard deviation = 0.57°C). For patient groups that were not treated with sedative and/or antishivering medications (6 groups), the average temperature difference between the actual and predicted drop was 0.0°C (standard deviation = 0.67°C), whereas groups that were treated with sedative and/or antishivering medications (5 groups), the average temperature difference between the actual and predicted drop was 0.53°C (standard deviation = 0.24°C). These data demonstrate that the reported core temperature responses to an infusion of cold saline are well within the predicted values of the present study, especially for the case in which no antishivering or sedative drugs are administered.

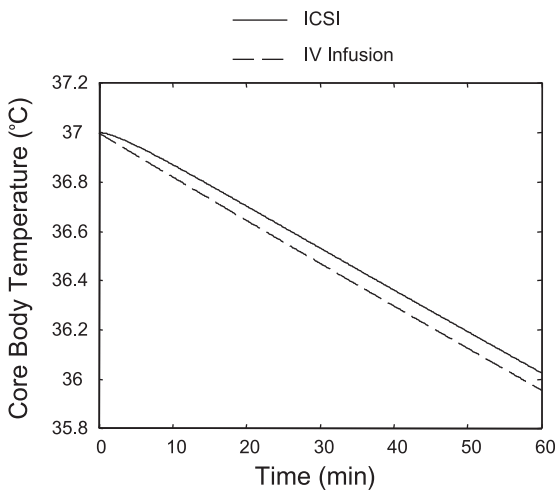

Fig. 6. Comparison of core body temperature for ICSI and intravenous (IV) infusion model.

Limitations of the model. The present model has several limitations: *1*) The intracranial anatomy was simplified. The geometry of the head was modeled as a hemisphere, but the real shape of the head is not exactly hemispherical. However, a careful selection of appropriate dimension yielded a brain volume of 1,285 ml, a value halfway between the average male and female brain (30). Moreover, the model omitted the dura matter and the cerebrospinal fluid (CSF). This layer was omitted because it is too thin (~2 mm), and the thermal properties of the CSF are very similar to those of the brain tissue (8, 38). *2*) The present model assumes constant and equal rates of heat transfer loss and heat generation inside the body. In reality, hypothermia-induced shivering will disturb this equilibrium and heat generation will exceed loss, resulting in a possible overestimation of body core cooling from the cooled jugular venous return. However, effective neuromuscular blockade in a clinical setting will counteract much of the effect of shivering. However, data from IV infusion studies (see above discussion) suggest that for modest temperature drops of 1–2°C, use of antishivering drugs is associated with temperature decreases greater than what would be theoretically predicted. However, in ICSI, brain temperatures would be considerably lower than core temperature, which might make shivering a greater factor. *3*) The Pennes equation describes a

continuum model where heat and mass transport are averaged over a representative unit volume. Continuum models are not able to predict the variation in temperature in the immediate vicinity of large, discrete blood vessels. However, the results obtained from a discrete vessel thermal model agreed well with Pennes's continuum model (49). *4*) The model assumes that temperature and hematocrit control the CBF independently. In theory, it is plausible, although not likely, that a reduced hematocrit may modify the cerebrovascular response to hypothermia, and vice versa. *5*) In the model it is assumed that the dependence of CBF on local temperature and hematocrit is the same as that for global temperature and hematocrit. Several animal experiments (25, 33, 50) have confirmed that there are not significant differences in the reduction of CBF between systemic cooling and selective brain cooling. Although, to the best of our knowledge, there are no similar studies investigating potential differences between local and systemic hemodilution, it is reasonable to assume that perfusion increases due to hemodilution are also locally mediated. Furthermore, a feline study has reported that vascular responses to oxygenation changes in the brain are locally mediated and occur within 3 s (34), suggesting that CBF dependence on local hematocrit should be the same as its dependence on global hematocrit.

APPENDIX

If a volume of fluid with volume V_{fluid}, density ρ_{fluid}, heat capacity c_{fluid}, and temperature T_{fluid} mixes and equilibrates with the body that has mass m_{body}, heat capacity c_{body}, and temperature T_{core}, the new body temperature is

$$T_{core\_new}\frac{V_{fluid}\rho_{fluid}c_{fluid}T_{fluid} + m_{body}c_{body}T_{core\_old}}{V_{fluid}\rho_{fluid}c_{fluid} + m_{body}c_{body}} \quad (A1)$$

If this volume is infused at rate F_{fluid}, then the body temperature is updated in this equation according to

$$T_{body}(t + \Delta t) = \frac{F\Delta t\rho_{fluid}c_{fluid}T_{fluid} + m_{body}c_{body}T_{body}(t)}{F\Delta t\rho_{fluid}c_{fluid} + m_{body}c_{body}} \quad (A2)$$

Equation A2 can be rearranged to

$$\frac{T_{body}(t + \Delta t) - T_{body}(t)}{\Delta t} = \frac{\rho_{fluid}c_{fluid}[T_{fluid} - T_{body}(t + \Delta t)]F_{fluid}}{m_{body}c_{body}} \quad (A3)$$

In the limit where $\Delta t \to 0$, *A3* is rewritten as

$$\frac{dT_{core}}{dt} = \frac{\rho_{fluid}c_{fluid}(T_{fluid} - T_{body})F_{fluid}}{m_{body}c_{body}} \quad (A4)$$

For *Eq. 18*, the fluid is the cold infused saline. For *Eq. 9*, the fluid is cold venous blood which returns from the brain. The rate of this flow is determined simply by integrating total blood perfusion throughout the brain model:

$$F_{venous} = \iiint_{Brain\ Model} \omega(\vec{r})d\vec{r} \quad (A5)$$

ACKNOWLEDGMENTS

The authors thank Dikla B. Neimark for assistance with the manuscript.

REFERENCES

1. **Badjatia N, Bodock M, Guanci M, Rordorf GA.** Rapid infusion of cold saline (4°C) as adjunctive treatment of fever in patients with brain injury. *Neurology* 66: 1739–1741, 2006.
2. **Baish JW.** Microvascular heat transfer. In: *The Biomedical Engineering Handbook* (2nd ed.), edited by Bronzio JD and Joseph D. Boca Raton, FL: CRC, 2000, p. 98-91–98-94.
3. **Baumgardner JE, Baranov D, Smith DS, Zager EL.** The effectiveness of rapidly infused intravenous fluids for inducing moderate hypothermia in neurosurgical patients. *Anesth Analg* 89: 163–169, 1999.
4. **Bernard S, Buist M, Monteiro O, Smith K.** Induced hypothermia using large volume, ice-cold intravenous fluid in comatose survivors of out-of-hospital cardiac arrest: a preliminary report. *Resuscitation* 56: 9–13, 2003.
5. **Cassot F, Zagzoule M, Marc-Vergnes JP.** Hemodynamic role of the circle of Willis in stenoses of internal carotid arteries. An analytical solution of a linear model. *J Biomech* 33: 395–405, 2000.
6. **Chen H, Chopp M, Zhang ZG, Garcia JH.** The effect of hypothermia on transient middle cerebral artery occlusion in the rat. *J Cereb Blood Flow Metab* 12: 621–628, 1992.
7. **Corbett RJ, Laptook AR.** Failure of localized head cooling to reduce brain temperature in adult humans. *Neuroreport* 9: 2721–2725, 1998.
8. **Diao C, Zhu L, Wang H.** Cooling and rewarming for brain ischemia or injury: theoretical analysis. *Ann Biomed Eng* 31: 346–353, 2003.
9. **Ding Y, Li J, Luan X, Lai Q, McAllister JP 2nd, Phillis JW, Clark JC, Guthikonda M, Diaz FG.** Local saline infusion into ischemic territory induces regional brain cooling and neuroprotection in rats with transient middle cerebral artery occlusion. *Neurosurgery* 54: 956–964; discussion 964–955, 2004.
10. **Eckmann DM, Bowers S, Stecker M, Cheung AT.** Hematocrit, volume expander, temperature, and shear rate effects on blood viscosity. *Anesth Analg* 91: 539–545, 2000.
11. **Enzmann DR, Ross MR, Marks MP, Pelc NJ.** Blood flow in major cerebral arteries measured by phase-contrast cine MR. *AJNR Am J Neuroradiol* 15: 123–129, 1994.
12. **Fahrig R, Nikolov H, Fox AJ, Holdsworth DW.** A three-dimensional cerebrovascular flow phantom. *Med Phys* 26: 1589–1599, 1999.
13. **Feigin V, Anderson N, Gunn A, Rodgers A, Anderson C.** The emerging role of therapeutic hypothermia in acute stroke. *Lancet Neurol* 2: 529, 2003.
14. **Fiala D, Lomas KJ, Stohrer M.** A computer model of human thermoregulation for a wide range of environmental conditions: the passive system. *J Appl Physiol* 87: 1957–1972, 1999.
15. **Frank SM, Cattaneo CG, Wieneke-Brady MB, El-Rahmany H, Gupta N, Lima JA, Goldstein DS.** Threshold for adrenomedullary activation and increased cardiac work during mild core hypothermia. *Clin Sci (Lond)* 102: 119–125, 2002.
16. **Frank SM, Higgins MS, Fleisher LA, Sitzmann JV, Raff H, Breslow MJ.** Adrenergic, respiratory, and cardiovascular effects of core cooling in humans. *Am J Physiol Regul Integr Comp Physiol* 272: R557–R562, 1997.
17. **Frank SM, Raja SN, Bulcao C, Goldstein DS.** Age-related thermoregulatory differences during core cooling in humans. *Am J Physiol Regul Integr Comp Physiol* 279: R349–R354, 2000.
18. **Georgiadis D, Schwarz S, Kollmar R, Schwab S.** Endovascular cooling for moderate hypothermia in patients with acute stroke: first results of a novel approach. *Stroke* 32: 2550–2553, 2001.
19. **Grathwohl KW, Bruns BJ, LeBrun CJ, Ohno AK, Dillard TA, Cushner HM.** Does hemodilution exist? Effects of saline infusion on hematologic parameters in euvolemic subjects. *South Med J* 89: 51–55, 1996.
20. **Greenfield RH, Bessen HA, Henneman PL.** Effect of crystalloid infusion on hematocrit and intravascular volume in healthy, nonbleeding subjects. *Ann Emerg Med* 18: 51–55, 1989.
21. **Harris BA, Andrews PJD.** Direct brain cooling. In: *Therapeutic Hypothermia*, edited by Mayer SA and Sessler DI. New York: Dekker, 2005, p. 323–386.
22. **Hillen B, Drinkenburg BA, Hoogstraten HW, Post L.** Analysis of flow and vascular resistance in a model of the circle of Willis. *J Biomech* 21: 807–814, 1988.
23. **Hoeks AP, Samijo SK, Brands PJ, Reneman RS.** Noninvasive determination of shear-rate distribution across the arterial lumen. *Hypertension* 26: 26–33, 1995.

23a. **Hendrikse J, van Raamt AF, van der Graaf Y, Mali WP, van der Grond J.** Distribution of cerebral blood flow in the circle of Willis. *Radiology* 235: 184–189, 2005.

24. **Holzer M, Bernard SA, Hachimi-Idrissi S, Roine RO, Sterz F, Mullner M; Collaborative Group on Induced Hypothermia for Neuroprotection After Cardiac Arrest.** Hypothermia for neuroprotection after cardiac arrest: systematic review and individual patient data meta-analysis. *Crit Care Med* 33: 414–418, 2005.

25. **Ibayashi S, Takano K, Ooboshi H, Kitazono T, Sadoshima S, Fujishima M.** Effect of selective brain hypothermia on regional cerebral blood flow and tissue metabolism using brain thermo-regulator in spontaneously hypertensive rats. *Neurochem Res* 25: 369–375, 2000.
26. **Johansen LB, Bie P, Warberg J, Christensen NJ, Hammerum M, Videbaek R, Norsk P.** Hemodilution, central blood volume, and renal responses after an isotonic saline infusion in humans. *Am J Physiol Regul Integr Comp Physiol* 272: R549–R556, 1997.
27. **Kammersgaard LP, Rasmussen BH, Jorgensen HS, Reith J, Weber U, Olsen TS.** Feasibility and safety of inducing modest hypothermia in awake patients with acute stroke through surface cooling: a case-control study: the Copenhagen Stroke Study. *Stroke* 31: 2251–2256, 2000.
28. **Kass LE, Tien IY, Ushkow BS, Snyder HS.** Prospective crossover study of the effect of phlebotomy and intravenous crystalloid on hematocrit. *Acad Emerg Med* 4: 198–201, 1997.
29. **Kim F, Olsufka M, Carlbom D, Deem S, Longstreth WT Jr, Hanrahan M, Maynard C, Copass MK, Cobb LA.** Pilot study of rapid infusion of 2 L of 4°C normal saline for induction of mild hypothermia in hospitalized, comatose survivors of out-of-hospital cardiac arrest. *Circulation* 112: 715–719, 2005.
30. **Koh I, Lee MS, Lee NJ, Park KW, Kim KH, Kim H, Rhyu IJ.** Body size effect on brain volume in Korean youth. *Neuroreport* 16: 2029–2032, 2005.
31. **Kollmar R, Schabitz WR, Heiland S, Georgiadis D, Schellinger PD, Bardutzky J, Schwab S.** Neuroprotective effect of delayed moderate hypothermia after focal cerebral ischemia: an MRI study. *Stroke* 33: 1899–1904, 2002.
32. **Konstas AA, Neimark MA, Laine AF, Pile-Spellman J.** A theoretical model of selective cooling using intracarotid cold saline infusion in the human brain. *J Appl Physiol* 102: 1329–1340, 2007.
33. **Laptook AR, Shalak L, Corbett RJ.** Differences in brain temperature and cerebral blood flow during selective head versus whole-body cooling. *Pediatrics* 108: 1103–1110, 2001.
34. **Malonek D, Grinvald A.** Interactions between electrical activity and cortical microcirculation revealed by imaging spectroscopy: implications for functional brain mapping. *Science* 272: 551–554, 1996.
35. **Martineau RJ.** Pro: a hematocrit of 20% is adequate to wean a patient from cardiopulmonary bypass. *J Cardiothorac Vasc Anesth* 10: 291–293, 1996.
36. **Mellergard P.** Changes in human intracerebral temperature in response to different methods of brain cooling. *Neurosurgery* 31: 671–677; discussion 677, 1992.
37. **Moore S, David T, Chase JG, Arnold J, Fink J.** 3D models of blood flow in the cerebral vasculature. *J Biomech* 39: 1454–1463, 2006.
38. **Nelson DA, Nunneley SA.** Brain temperature and limits on transcranial cooling in humans: quantitative modeling results. *Eur J Appl Physiol* 78: 353–359, 1998.
39. **Pennes HH.** Analysis of tissue and arterial blood temperature in the resting human forearm. *J Appl Physiol* 1: 93–122, 1948.
40. **Rajek A, Greif R, Sessler DI, Baumgardner J, Laciny S, Bastanmehr H.** Core cooling by central venous infusion of ice-cold (4 degrees C and 20 degrees C) fluid: isolation of core and peripheral thermal compartments. *Anesthesiology* 93: 629–637, 2000.
41. **Schwab S, Georgiadis D, Berrouschot J, Schellinger PD, Graffagnino C, Mayer SA.** Feasibility and safety of moderate hypothermia after massive hemispheric infarction. *Stroke* 32: 2033–2035, 2001.
42. **Schwartz AE, Stone JG, Pile-Spellman J, Finck AD, Sandhu AA, Mongero LB, Michler RE.** Selective cerebral hypothermia by means of transfemoral internal carotid artery catheterization. *Radiology* 201: 571–572, 1996.
43. **Slotboom J.** Localized therapeutic hypothermia in the brain for the treatment of ischemic stroke. *J Appl Physiol* 102: 1303–1304, 2007.
44. **Slotboom J, Kiefer C, Brekenfeld C, Ozdoba C, Remonda L, Nedeltchev K, Arnold M, Mattle H, Schroth G.** Locally induced hypothermia for treatment of acute ischaemic stroke: a physical feasibility study. *Neuroradiology* 46: 923–934, 2004.
45. **Stamler KD.** Effect of crystalloid infusion on hematocrit in nonbleeding patients, with applications to clinical traumatology. *Ann Emerg Med* 18: 747–749, 1989.
46. **Sukstanskii AL, Yablonskiy DA.** Theoretical limits on brain cooling by external head cooling devices. *Eur J Appl Physiol* 101: 41–49, 2007.
47. **Tanaka H, Fujita N, Enoki T, Matsumoto K, Watanabe Y, Murase K, Nakamura H.** Relationship between variations in the circle of Willis and flow rates in internal carotid and basilar arteries determined by means of magnetic resonance imaging with semiautomated lumen segmentation: reference data from 125 healthy volunteers. *AJNR Am J Neuroradiol* 27: 1770–1775, 2006.
48. **Van Laar PJ, Hendrikse J, Golay X, Lu H, van Osch MJ, van der Grond J.** In vivo flow territory mapping of major brain feeding arteries. *Neuroimage* 29: 136–144, 2006.
49. **Van Leeuwen GM, Hand JW, Lagendijk JJ, Azzopardi DV, Edwards AD.** Numerical modeling of temperature distributions within the neonatal head. *Pediatr Res* 48: 351–356, 2000.
50. **Walter B, Bauer R, Kuhnen G, Fritz H, Zwiener U.** Coupling of cerebral blood flow and oxygen metabolism in infant pigs during selective brain hypothermia. *J Cereb Blood Flow Metab* 20: 1215–1224, 2000.
51. **Wang H, Olivero W, Lanzino G, Elkins W, Rose J, Honings D, Rodde M, Burnham J, Wang D.** Rapid and selective cerebral hypothermia achieved using a cooling helmet. *J Neurosurg* 100: 272–277, 2004.
52. **Wysocki M, Andersson OK, Persson B, Bagge U.** Vasoconstriction during acute hypervolemic hemodilution in hypertensive patients is not prevented by calcium blockade. *Angiology* 49: 41–48, 1998.
53. **Wysocki M, Persson B, Aurell M, Braide M, Bagge U, Andersson OK.** Haemodynamic and haemorheological effects of hypervolaemic haemodilution in men with primary hypertension. *J Hypertens* 5: 185–189, 1987.
54. **Xu X, Tikuisis P, Giesbrecht G.** A mathematical model for human brain cooling during cold-water near-drowning. *J Appl Physiol* 86: 265–272, 1999.
55. **Zhu L, Diao C.** Theoretical simulation of temperature distribution in the brain during mild hypothermia treatment for brain injury. *Med Biol Eng Comput* 39: 681–687, 2001.
56. **Zhu M, Ackerman JJ, Sukstanskii AL, Yablonskiy DA.** How the body controls brain temperature: the temperature shielding effect of cerebral blood flow. *J Appl Physiol* 101: 1481–1488, 2006.